From July 2009 *High Frequency Electronics*


# Adjustable Gain Cascode Low Noise Amplifier

**By Chin-Leong Lim**
**Avago Technologies**

This article describes the design and performance of an EPHEMT low noise amplifier MMIC and its evaluation circuit

Tower mounted amplifiers (TMA) serve to lower the system noise figure (NF) in cellular base-stations. For performance reasons, the TMA is located as near to the receiving aerial as practical and has to be connected to the rest of the radio at the tower's base by a long run of coaxial cable. The parameters critical to TMA performance are low NF for reasons of optimizing coverage area, high gain to overcome the cable loss, and high linearity as the TMA must operate reliably in a crowded RF spectrum. Additionally, the TMA is required to present a nonreflective input and output terminations, that is, a return loss (RL) of –20 dB, and yet exhibits sub-1 dB NF. LNA designs for TMA service typically rely on the hybrid-coupled balanced amplifier arrangement to satisfy this challenging combination of noise and RL requirements [1]. Unfortunately, the balanced amplifier approach increases the cost, size and power consumption of the LNA. The MMIC device described henceforth (Avago Technologies MGA-632P8) represents an important milestone for cellular TMA designs as it simultaneously achieves both target RL and NF without relying on costly and space-hogging hybrid couplers (also known as quadrature hybrids). A means for varying the gain is provided to fulfill customers' requirement for gain leveling between adjacent bands, e.g., at PCS and WCDMA.

## Device and Packaging Design

The semiconductor technology that forms the basis of this MMIC is EPHEMT structures on a GaAs wafer; a combination that enables the lowest noise figure of all RF technologies at a reasonable cost [2]. A half micron gate length was chosen as a compromise between high frequency performance and manufacturability and yield [3]. This process has a nominal gain product bandwidth ($f_T$) of ~30 GHz.

The cascode topology was chosen for this design as it offers improved gain and isolation over a common emitter (CE) amplifier [4]. A single CE stage is not expected to have enough gain to overcome the noise figure of successive stages [5], and the gain shortfall will be most acutely felt at the higher cellular bands such as PCS and UMTS. Although a cascade of two CE stages can similarly boost the gain, the cascode is a more power efficient approach as the same bias current is shared by both transistors (Q1 and Q2) in the latter arrangement [5]. The cascode configuration consists of a CE stage Q1 driving a Common Base (CB) 2nd stage Q2. Q2 has an input impedance of [3]

$$Z_{in\_Q2} \approx 1/g_m$$

Where, $g_m$ is the forward transconductance. As Q1's load is essentially the input impedance of Q2,

$$R_{L\_Q1} = Z_{in\_Q2} = 1/g_m$$

So, gain of Q1 is [6]

$$A_{v\_Q1} = -g_m.R_L = -g_m Z_{in\_Q2} = -1$$

This demonstrates that the heavy loading by $Z_{in\_Q2}$ reduces Q1's voltage gain to unity. Consequently, the cascode achieves a higher

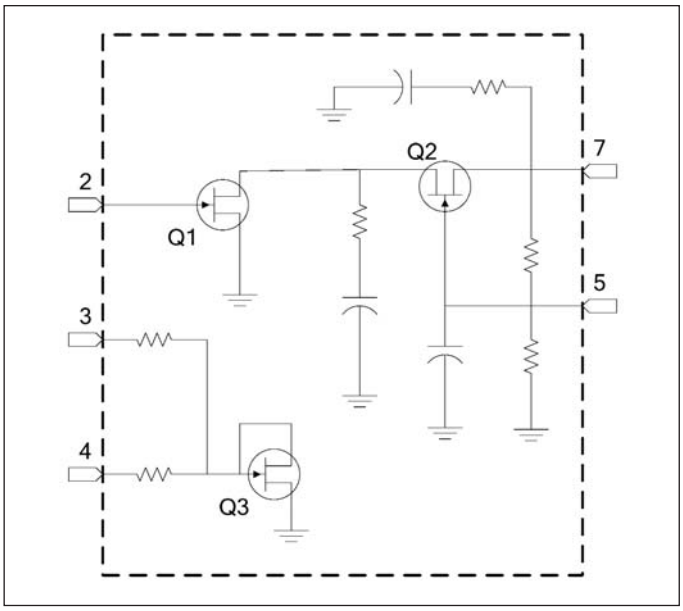


**Figure 1 · Simplified circuit of the MMIC.**

gain than the common emitter amplifier, particularly at high frequencies, by elimination of the Miller effect [7].

The LNA stage is usually followed by an image rejection filter. Both the aerial and the post-LNA filter are narrow-band components and their guaranteed characteristics (e.g. frequency response) are very termination-sensitive. In a non-unilateral device (i.e., $S_{12} \neq 0$) such as a microwave LNA, any change in the load impedance is also transferred back to the input port, and vice versa. As a result, detuning of either the filter or the aerial can occur due to the mutual interaction between the source and load impedances. The cascode connection has better reverse isolation than a CE amplifier, and this property is prized in LNA designs for the reasons discussed in the measurement section. When the reverse transmission coefficient $S_{12}$ approaches zero, the $S_{11}$ becomes insensitive to load changes as shown by the following expression

$$S'_{11} = S_{11} + \frac{S_{12}S_{21}\Gamma_L}{1 - S_{22}\Gamma_L} \approx S_{11}$$

(when $S_{12} \rightarrow 0$).

In the same manner, $S'_{22}$ will also approximate $S_{22}$ if $S_{12}$ is small. In practical numbers, the cascode amplifier's $y_{12}$ has been reported to be 1/200 to 1/2000 of a CE stage with the same DC bias current [8].

The enhancement mode technology provides superior performance while allowing direct DC grounding of the transistor's source terminal. This also greatly simplifies the power supply requirement as the entire amplifier can be powered using a single polarity voltage supply.

The FET device's threshold voltage, $g_m$, and $R_{DS}$(on) can shift with temperature—therefore, a good bias circuit should vary accordingly with temperature to maintain the same operating point. The gate-source junction of Q3 functions as a voltage reference for Q1's gate bias. As both Q1 and Q3 undergo the same semiconductor processing and also share the same thermal environment, the latter can function as "like material" reference to compensate for thermal effects [9]. By having their drain currents "track" one another, the Q1 and Q3 pair acts like a "current mirror" [10]. This also takes care of the spread of $V_{GS}$ values required to cope with batch-to-batch variation in $g_m$.

The die is packaged into a miniature 2 by 2 mm leadless package using bond-wires as interconnects. At the center of the package's bottom surface, a large ground contact is straddled by two rows of leads. The ground contact's large surface area provides efficient heat transfer to the PCB and also low inductance RF grounding. The thermal path is very short as the MMIC die rests directly on this ground contact. The result is a package with a junction-to-case thermal resistance ($\theta_{jc}$) of 47 ºC/W. A low $\theta_{jc}$ is desirable from both performance and reliability perspectives— parametric drift that is a consequence of device heating is minimized and the Mean Time to Failure (MTTF) is extended when the junction runs cooler [11, 12].

## Application Design

The application circuit provides the external matching and biasing components that were not feasible to integrate at the dice level. The input network consisting of C1 and L1 provides a match to Q1's input and also impart a high pass characteristic to roll off undesirable gain below the operating frequency. L1 is chosen for a high unloaded $Q$ ($Q_u$) and a Self Resonant Frequency (SRF) that is higher than the operating frequency because signal loss in the 1st stage (i.e., the LNA) has the greatest effect on the overall system noise figure, as indicated by the Friss equation [13]

$$F = F_1 + \frac{F_2 - 1}{G_1} + \frac{F_3 - 1}{G_1 G_2} + \ldots$$

and, moreover, the lost signal cannot be recovered by processing further downstream. The insertion loss of a single transmission resonator is represented by [14]

$$L(f) = -10\log\left[\frac{1 + \left(2Q_l \frac{f - f_0}{f_0}\right)^2}{\left[1 - \left(\frac{Q_l}{Q_u}\right)\right]^2}\right]$$

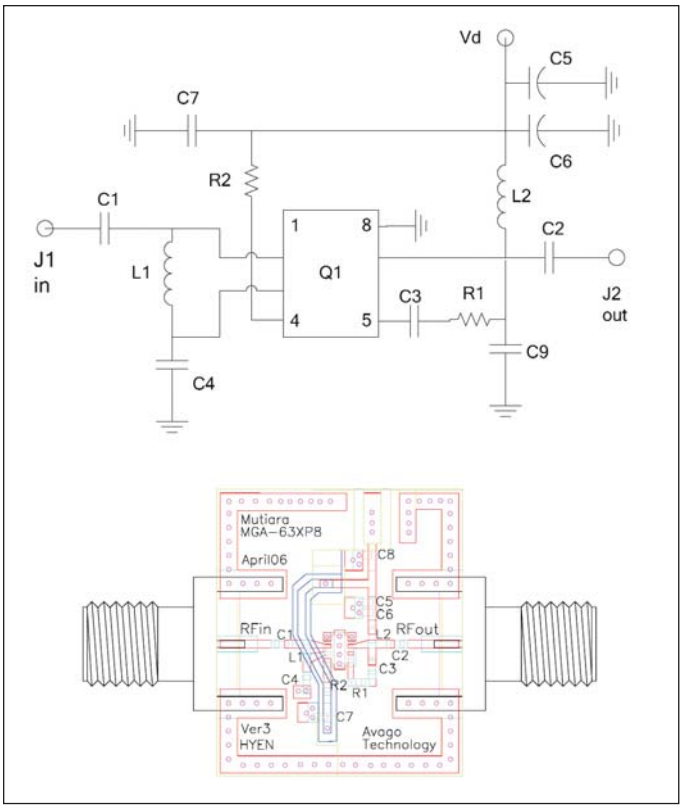


**Figure 2 · Application circuit and PCB layout.**

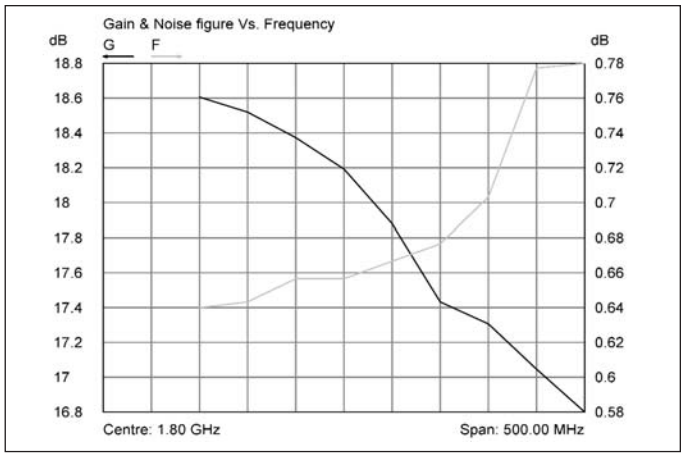


**Figure 3 · Gain and noise figure vs. frequency.**

and, substituting $f = f_0$ in the case of a filter network that is matched to the LNA at the design frequency $f_0$, reduces the equation to

$$loss = 20\log\frac{Q_u - Q_l}{Q_u}$$

The output of the cascode amplifier is matched to the load by the combination of L2 and C2. Again, high pass network was used to reduce the gain below the design frequency. An additional bonus of the high pass topology is the saving of one component as the shunt inductor (L2) also serves at the bias insertion network in conjunction with C5 and C6. The output shunt capacitor C9 is essential for stability in the X-band region, and its role is described in greater detail in the next section. R1 and C3 channel part of the output signal back to the base of Q2. This local negative feedback around Q2 is intended for gain leveling between adjacent bands, such as PCS and WCDMA. Local feedback around the CB stage, as opposed to global feedback, keeps the NF constant. R1's nominal value is 160R—increasing R1 from a minimum value of 62R to a maximum of 22k will reduce the gain correspondingly from 18.5 to 16.2 dB at 1.9 GHz. Additionally, the negative feedback around the CB stage also stabilizes the amplifier in the upper microwave region; without this RC network, the Rollett stability factor ($k$) can drop below unity in the 8 ~ 14 GHz region depending on PCB layout. R2 controls the current flowing through the voltage reference half of the current mirror. Varying the value of R2 allows the user to program the device's current consumption.

The PCB is made from 10 mil Rogers RO4350 substrate. An FR4 substrate is used as backing material to provide mechanical rigidity and to increase the overall thickness to 0.8 mm to suit standard edge launched coax transitions. RF connections to the demoboard are made via edge-mounted microstrip to SMA coax transitions. The application board is powered from a single 4.0 V power supply and the current drain is approximately 60 mA.

## Measurement and Discussion

Although the application of this MMIC at various frequencies (e.g., 1.5, 1.8 and 2.6 GHz) have been demonstrated [15], this paper limits itself to the results of the 1.8 GHz version. This frequency is representative of PCS base-station application—the expected biggest market segment for this MMIC.

The performance parameters critical for winning customer acceptance are low noise figure (NF) and good return loss over a broad bandwidth. The application circuit ably achieves the first goal by demonstrating a sub 0.7 dB NF at the design frequency. As the test-board and connectors losses were not subtracted from the measured result, the device-only NF is plausibly estimated to be in the 0.4 ~ 0.5 dB range. All the measurements are made on a prototype built with low-cost ceramic-core wire-wound chip inductor (Coilcraft 0402CS series) in the matching networks. It is reasonable to expect even lower NF if air-core spring wound inductors are used instead.

The design goal was to create a single-ended MMIC amplifier that is capable of achieving the same superior RL of the balanced amplifier, but without the attendant

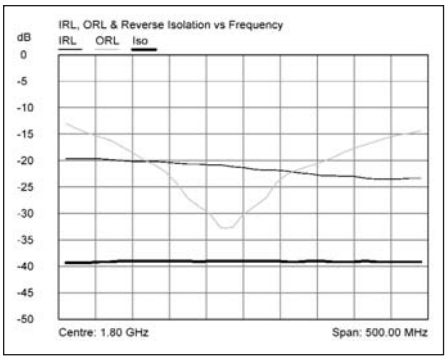


**Figure 4 · Input and output return loss and reverse isolation vs. frequency.**

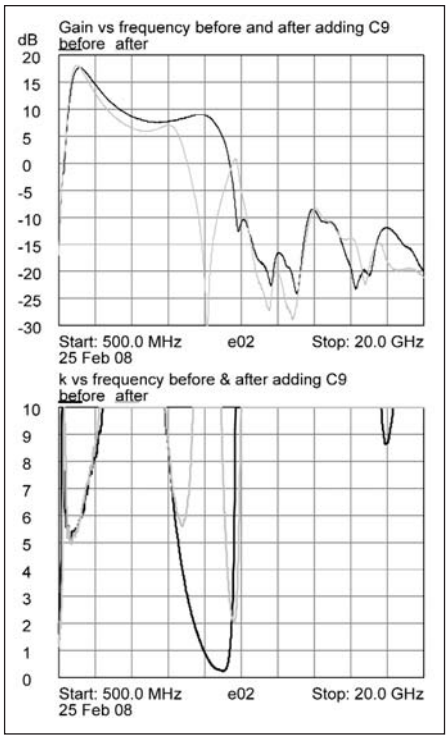


**Figure 5 · (a) Wideband gain and (b) Rollett stability factor k before and after addition of output shunt capacitor C9.**

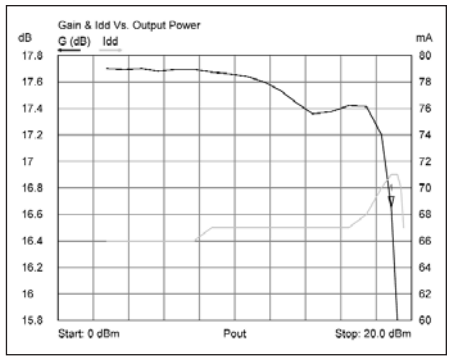


**Figure 6 · Gain and current vs. output power.**

size and cost trade-offs. The application prototype clearly attains the target –20 dB input and output return losses over a wide bandwidth. The excellent input and output match lessens the effect of detuning when the LNA is cascaded with other stages in the RF chain. For example, filters and aerials are especially susceptible to the adverse effects of reflective terminations. Designing the amplifier's input and output for a close match to 50 ohms over the operating bandwidth, prevents unpredictable shift in the filter's frequency response. Troublesome interaction between the aerial and post-LNA filter is minimized by the LNA's almost –40 dB of reverse isolation; the previously discussed claim of the cascode superior isolation over a single CE stage is thus practically validated. Direct Conversion Receivers (DCR) also stand to benefit from the cascode's better reverse isolation [16]. High isolation in the LNA suppresses the local oscillator to RF leakage that is responsible for DC offset errors in the DCR architecture [17].

High-pass networks are used for the input and output matching to roll-off excessive gain at low frequency (LF), i.e., the tens of MHz range. As the Rollett stability factor

$$k = (1 + |S_{11}S_{22} - S_{12}S_{21}|^2 - |S_{11}|^2 - |S_{22}|^2) / (2\,|S_{12}S_{21}|)$$

computed from the measured *S*-parameters satisfies the ≥ 1 criterion, the evaluation circuit is considered unconditionally stable for all possible source and load terminations of positive real part.

While the aforementioned high pass networks are adequate to ensure unconditional stability from LF up to the design frequency, inadequate stability margin far above the pass-band requires different stabilization techniques. Inadvertent input-output coupling and component self-resonances are the usual suspects for these oscillation tendencies at the upper microwave region. For example, if there are pronounced peaks in the frequency response above the pass-band, the amplifier may oscillate under a certain unfavorable combination of environmental conditions [18], e.g., when the enclosure's cavity resonance coincides with the gain peak [19]. In the first iteration of the application circuit, which did not incorporate the output shunt capacitor C9, a gain peak unexpectedly occurred around ~8-9 GHz. A direct consequence of this gain peak is the *k* stability factor dropping below 1 in the affected frequency range. This can be remedied by shunting the LNA output with a small value capacitor (C9). See Figure 5.

In third generation (3G) cellular systems such as WCDMA, the requirement for simultaneous transmission and reception increases the linearity demand on the receiver front-end. In a base-station employing Frequency Domain Duplexing (FDD), the conventional transmit-receive switch separating the transmitter from the receiving side is replaced by a duplexer. Unfortunately, the duplex filters typically afford poorer isolation than a switch, and this allows a significant portion of the transmit power to leak into the receiver's front end [20]. If the LNA has poor "blocking" performance, the small signal will compress faster than the larger leakage power—causing a desensitizing of the receiver [21]. The challenge that this leaked power poses to LNA linearity is further magnified by the typical 12 dB peak-to-average power ratio (PAR) of a multi-carrier hybrid-QPSK transmission [22].

The 1 dB gain compression point, $P_{1dB}$, which indicates the upper limit

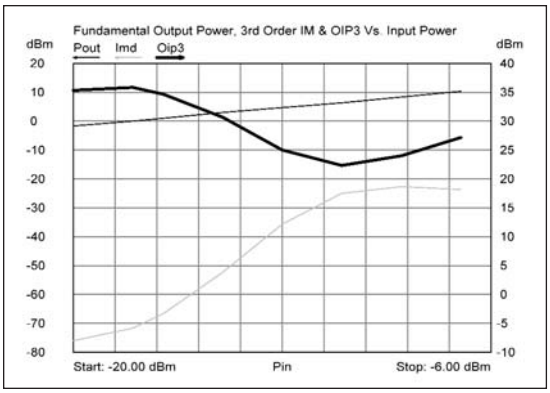


**Figure 7 · Fundamental output, 3rd order IM and OIP3 vs. input power.**

| *Parameter* | *Frequency (GHz)* | | |
|---|---|---|---|
| | *1.8/1.9* | *1.5* | *2.6* |
| G (dB) | 17.5 | 18 | 15 |
| F (dB) | 0.7 | 0.7 | 0.9 |
| RL (dB) | < –20 | < –25 | < –25 |
| $P_{1dB}$ | 18.9 | n.a | n.a |
| $IIP_3$ | 17.5 | 17 | 20 |
| $OIP_3$ | 35 | 35 | 35 |
| Test Conditions: $V_d$ = 4.0 V, $I_d$ = ~60 mA | | | |

**Table 1 · Typical measured performance values for the MGA-632P8 EPHEMT LNA MMIC.**

of either the input or the output power level at which saturation has started to occur in the LNA, is useful as a figure of merit for gauging the device's ability to resist desensitization by in-band blockers [23]. This application example has an output $P_{1dB}$ of 18.9 dBm (Fig. 6).

The intercept point is another measure of amplifier linearity. The theoretical point when the fundamental signal and the third order intermodulation distortion are of equal amplitude is the third order intercept point, IP3. The distortion level at other power levels can be conveniently calculated from the amplifier's IP3 specification. Referenced to the output,

$$OIP_3 = P_{fund} + \frac{\Delta IM}{2}$$

where $P_{fund}$ is the amplitude of either one of the fundamental outputs, and $\Delta IM$ is the amplitude difference between the fundamental tones and the intermodulation products.

Using two –20 dBm input tones spaced 5 MHz apart, the OIP3 is approximately 35 dBm.

In a linearity contest among the mature RF process technologies already in wide usage, GaAs PHEMT is the undisputed leader [24]. The linearity efficiency of RF amplifiers is commonly compared using the Linearity Figure of Merit (LFOM). It is defined as [24]:

$$LFOM = OIP_3 - P_{1dB}$$

Calculating for this device,

$$LFOM = 35\ dBm - 18.9\ dBm \approx 16\ dB$$

The proprietary GaAs PHEMT process flavor confers a linearity efficiency advantage that is clearly ahead of the 10 dB LFOM value typically reported for the HEMT family [25].

The nominal performance of the application circuit at various frequencies is summarized in Table 1.

## Conclusion

This cascode amplifier MMIC is eminently suitable for adoption in the LNA design slot of performance-critical base-stations and other wireless infrastructures in the L- and S-bands. Its value propositions are an industry-leading noise and linearity performance, a return loss performance as good as balanced amplifiers but without the latter's space and cost penalties, and a low cost plastic package that is both space saving and thermally efficient.

## Acknowledgement

The author thanks M. Sharifah, H. Nazri, S. C. Goh, C. C. Loh, M. Fuad, C. S. Teoh, and K. O. Yap for their help at different stages of this project.

## Author Information

Chin-Leong Lim is factory application engineer for RF diodes, discrete transistors and MMICs at Avago Technologies in Penang, Malaysia. Prior to joining Avago in 1997, he was design engineer at Robert Bosch in Penang for 7 years. There he designed automotive broadcast-band receivers and set up the EMC test facility. He has authored 10 papers and is a senior member of IEEE. He received the B.Tech. degree in electrical engineering from Universiti Teknologi Malaysia, Kuala Lumpur in 1990. His interests include radio receiver and PIN diode circuits. He can be reached by e-mail at: chin-leong.lim@avagotech.com

## References

1. T. Chong, "A Low-Noise, High-Linearity Balanced Amplifier in Enhancement-mode GaAs pHEMT Technology for Wireless Base-Stations," *Proceedings of the European Microwave Conference,* 2005.

2. O. Berger, "GaAs MESFET, HEMT and HBT Competition with Advanced Si RF Technologies," *Digest of The International Conference on Compound Semiconductor Manufacturing Technology,* 1999, Vancouver, Canada.

3. S. A. Mass, "Solid State Devices," in *The RF and Microwave Design Cookbook,* Artech House,

Norwood, MA, 1998, pp. 83.

4. "FETs for Video Amplifiers," Application Note A70-2, Siliconix.

5. C. Baringer, and C. Hull, "Amplifiers for Wireless Communications," in *RF And Microwave Circuit Design for Wireless Communications,* Ed. L. E. Larson, Artech House, Norwood, MA, 1997.

6. U. Tietze, and C. Schenk, "Broadband Amplifiers," in *Advanced Electronic Circuits,* Springer-Verlag, New York, 1978, pp. 139-140.

7. P. Horowitz, and W. Hill, *The Art of Electronics,* 2nd edition, Cambridge University Press, 1989, pp. 102-103.

8. U. L. Rohde, and T.T.N. Bucher, "Amplifiers and Gain Control," in *Communication Receivers: Principles and Design,* McGraw-Hill Book Co., Singapore, 1994, pp. 220.

9. C. Blair, "Biasing LDMOS FETs for Linear Operation," *Applied Microwave & Wireless,* Jan. 2000, pp. 90-94.

10. R. Marston, "Constant Currrent Generator Circuits," *Electronics Today International,* May 1981, pp. 40-43.

11. R. W. Waugh, "Diode Reliability," presented at the Hewlett Packard Diode Seminar, Spring 1999.

12. J. P. Silver, *Component Reliability Tutorial* [Online]. Available at: http://www.rfic.co.uk.

13. "Fundamentals of RF and Microwave Noise Figure Measurements," Application Note 57-1, Agilent Technologies, Inc. Available at: http://www.agilent.com.

14. K. V. Puglia, "A General Design Procedure for Bandpass Filters Derived From Low Pass Prototype Elements: Part I," *Microwave Journal,* Dec. 2000, pp. 28.

15. MGA-632P8 Low Noise, High Linearity Active Bias Low Noise Amplifier Datasheet. Available at: http://www.avagotech.com.

16. J. Laskar, B. Matinpour, and S. Chakraborty, "Silicon Based Receiver Design," in *Modern Receiver Front-Ends,* John Wiley & Sons, Inc., New Jersey, 2004, pp. 55.

17. A. A. Abidi, "Low Frequency Radio Frequency ICs for Portable Communications," in *RF And Microwave Circuit Design for Wireless Communications,* Ed. L. E. Larson, Artech House, Norwood, MA, 1997.

18. A. J. Ward, "Appendix I: Determining the optimum amount of source inductance," in *High Intercept Low Noise Amplifier for the 1930 - 1990 MHz PCS Band using the Agilent ATF-34143 Low Noise PHEMT,* Avago Technologies Application Note 1191, Nov. 1999.

19. A. J. Ward, "Successful Low Noise Amplifier Design," *RF / Wireless Design Seminar,* Spring 1998, Hewlett Packard Co., pp. 22-25.

20. O. K. Jensen, et al, "RF Receiver Requirements for 3G W-CDMA Mobile Equipment," *Microwave Journal,* February 2000, pp. 24.

21. W. Domino, N. Vakilian, and D. Agahi, "Polynomial Model of Blocker Effects on LNA/Mixer Devices," *Applied Microwave & Wireless,* Jun. 2001, pp. 30-38.

22. M. Yu, "Power-handling capability for RF filters," *IEEE Microwave Magazine,* Oct. 2007, pp. 88-97.

23. R. E. Watson (1987, April), *Receiver Dynamic Range: Part 1* [Online], 14(2). Available at: http://www.wj.com.

24. R. S. Pengelly, "Improving the Linearity and Efficiency of RF Power Amplifiers," *High Frequency Electronics,* September 2002, pp. 26.

25. T. Nguyen (2005, January 18), *Choosing the Proper RF Amplifier Based on System Requirements* [Online]. Available at: http://www.wj.com/documents/Articles_PDF/.